

# Evidence for an InterMediate Line Region in AGN's Inner Torus Region and Its Evolution from Narrow to Broad Line Seyfert I Galaxies

Ling Zhu<sup>1</sup>, Shuang Nan Zhang<sup>1,2,3</sup>, and Sumin Tang<sup>4</sup>

<sup>1</sup>Department of Physics and Tsinghua Center for Astrophysics, Tsinghua University, Beijing 100084, China; zhul04@mails.tsinghua.edu.cn, zhangsn@tsinghua.edu.cn

<sup>2</sup>Key Laboratory of Particle Astrophysics, Institute of High Energy Physics, Chinese Academy of Sciences, P.O. Box 918-3, Beijing 100049, China

<sup>3</sup>Physics Department, University of Alabama in Huntsville, Huntsville, AL 35899, USA

<sup>4</sup>Harvard-Smithsonian Center for Astrophysics, 60 Garden St, Cambridge, MA 02138, USA

## ABSTRACT

We have decomposed the broad H $\alpha$ , H $\beta$  and H $\gamma$  lines of 90 Active Galactic Nuclei (AGNs) into a superposition of a very broad and an intermediate Gaussian components (VBGC and IMGC) and discovered that the two Gaussian components evolve with FWHM of the whole emission lines. We suggest that the VBGC and the IMGC are produced in different emission regions, namely, Very Broad Line Region (VBLR) and Intermediate Line Region (IMLR). The details of the two components of H $\alpha$ , H $\beta$  and H $\gamma$  lines indicate that the radius obtained from the emission line reverberation mapping normally corresponds to the radius of the VBLR, but the radius obtained from the infrared reverberation mapping corresponding to IMLR, i.e., the inner boundary of the dusty torus. The existence of the IMGC may affect the measurement of the black hole mass in AGNs. Therefore, the deviation of NLS1s from the M-sigma relation may be explained naturally in this way. The evolution of the two emission line regions may be related to the evolutionary stages of the broad line regions of AGNs from NLS1s to BLS1s. Other evidences for the existence of the IMLR are also presented.

**Key words:** line: profiles; quasars: emission lines; galaxies: structure; Galaxy: evolution; galaxies: active; galaxies: nuclei

## 1 INTRODUCTION

Type I AGNs are often classified into two subclasses according to the Full Width at Half Maximum (FWHM) of their broad H $\beta$  lines, i.e NLS1 and BLS1. There is a tight correlation between the black hole mass and the stellar velocity dispersion of the bulge of normal galaxies, the so called M-sigma relation (e.g. Magorrian et al. 1998; Tremaine et al. 2002;). BLS1s are found also to follow this relation well (Greene & Ho 2005). However, NLS1s seem to deviate from this relation; they seem to have much smaller masses or much higher stellar velocity dispersions (e.g., Wang & Lu 2001; Zhou et al. 2006). We call this *under-massive black hole problem of NLS1s*. It is not clear if the luminosity dependence of dust torus and broad line region is simultaneously related to the under-massive black hole problem and the receding torus model that used to explain the luminosity function of AGN (Simpson 2005). Progress towards solving these problems may shed new lights to the understanding the hierarchical evolution of AGN and its host galaxy, as

well as the feeding, fueling and growth of supermassive black holes. In this paper we attempt to address both problems in a coherent way by studying a sample of SDSS AGNs with strong broad emission lines.

## 2 LINE DECOMPOSITION AND STATISTICAL ANALYSIS

The sample contains 90 objects with clear H $\alpha$ , H $\beta$ , and H $\gamma$  line profiles that can be decomposed. They are selected by La Mura et al (2004) from SDSS 3 based on their balmer line intensities. 21 of them are classified as NLS1s. A double Gaussian component model, i.e IMGC and VBGC can fit the broad line very well. H $\alpha$ , H $\beta$  and H $\gamma$  lines are fitted with their FWHM fixed with each other; a deviation of 10% are allowed. Several decomposition samples are presented in Fig.1. The statistical analysis are presented in Fig.2. H $\alpha$ , H $\beta$  and H $\gamma$  lines behave similarly. Our analysis is focused on H $\beta$ . The FWHM ratios range from 1.5 to 4 in the NLS1 group

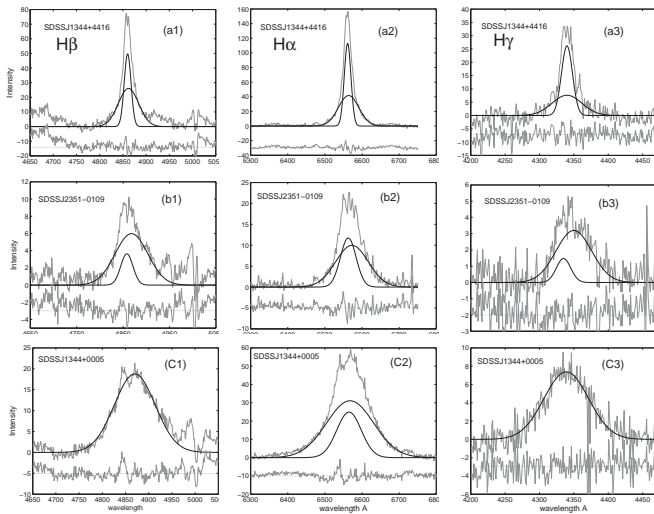


**Figure 1.** Decomposition example of broad H $\beta$ , H $\alpha$  and H $\gamma$  lines. From (a) to (c), FWHM of the line increases, and the IMGC becomes weaker and may disappear sometimes, e.g., in subpanels c1 & c3. Note that for in subpanel c2, the IMGC of H $\alpha$  line is still detectable, in contrast to H $\beta$  and H $\gamma$  lines, because the intermediate component of H $\alpha$  is normally much stronger than H $\beta$  and H $\gamma$  lines.

which lie on the left of Fig.2(a1). The intensity ratio of the very broad Gaussian component to the whole line is about 0.6 in these objects. This means that for NLS1s the intermediate Gaussian component has an intensity comparable to the very broad one, and consequently the FWHM of the whole line of NLS1s is dominated by the intermediate Gaussian component. With FWHM increasing, the intermediate Gaussian component becomes weaker and finally disappears, which can be seen from Fig.2(b1). The whole line can be simply described by a single very broad Gaussian component when FWHM reaches about 5000 km·s<sup>-1</sup>. In Fig.2(c1), FWHM ratio of the intermediate Gaussian component to the very broad Gaussian component becomes larger with increasing FWHM.

### 3 BHM CORRECTION

Reverberation-based black hole mass is calculated by the virial equation

$$M_{\text{BH}} = \frac{R_{\text{BLR}}}{G} f^2 \text{FWHM}_{\text{H}\beta}^2, \quad (1)$$

where  $\text{FWHM}_{\text{H}\beta}$  is the FWHM of the whole H $\beta$ , which represents the virial velocity of the BLR. For an isotropic velocity distribution, as generally assumed,  $f = \sqrt{3}/2$ .  $R_{\text{BLR}}$  is the BLR radius obtained by reverberation mapping, which is related to an AGN's continuum luminosity by the empirical Radius-Luminosity relation (Bentz et al. 2006):

$$\log \frac{R_{\text{BLR}}}{\text{lt} - \text{days}} = (0.518 \pm 0.039) \log \frac{\lambda L_{\lambda}(5100\text{\AA})}{\text{erg} \cdot \text{s}^{-1}} - 21.2 \pm 1.7. \quad (2)$$

This relation has been starlight-corrected. We use this equation to calculate  $R_{\text{BLR}}$  throughout this work. Because reverberation mapping is used to measure the radius of the broad line region, naturally it normally measures the radius

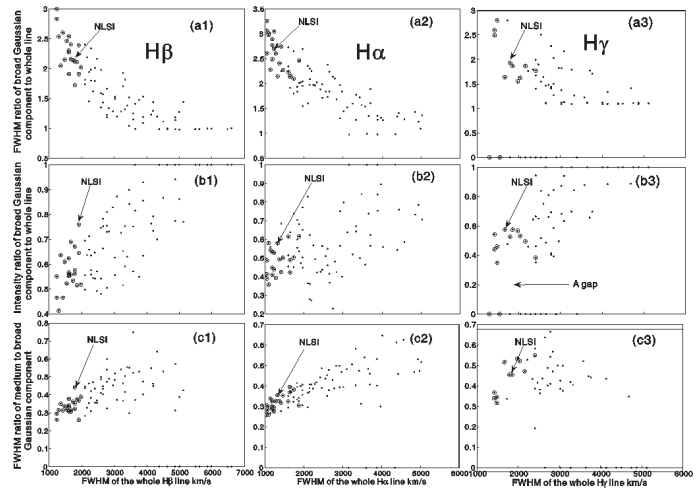


**Figure 2.** Statistical analysis of broad H $\beta$ , H $\alpha$  and H $\gamma$  lines. With the FWHM increasing, FWHM ratio of VBGC to the whole line becomes smaller and finally reaches unity, the intensity ratio of the VBGC to the whole line becomes larger and finally also reaches unity, and the IMGC becomes broader and weaker.

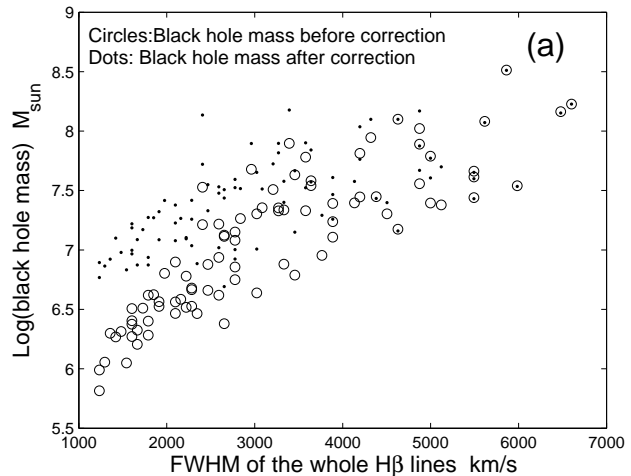


**Figure 3.** Black hole masses (in units of solar mass  $M_{\odot}$ ) are plotted in logarithm scale. Circles are black hole mass calculated with equation (1). Dots are that after correction using equation (3). Clearly the correction is more effective for AGNs with smaller FWHM, i.e., NLS1s.

of the inner most emission line region, i.e. the VBLR in our analysis. Consequently, FWHM of the very broad Gaussian component, instead of FWHM of the whole line, should be used to calculate the black hole mass. We therefore correct the black hole mass in this way:

$$M_{\text{BHb}} = \frac{R_{\text{VBLR}}}{G} f^2 \text{FWHM}^2 \left( \frac{\text{FWHMb}}{\text{FWHM}} \right)^2, \quad (3)$$

where FWHMb is the FWHM of the very broad Gaussian component, and  $R_{\text{VBLR}}$  is taken as the  $R_{\text{BLR}}$  in the R-L relation. It gives a more significant mass correction for NLS1s than for BLS1s as shown in Fig.3. After such correction, NLS1s still have smaller black hole masses but normal accretion rate in units of the Eddington rate. Fifteen objects in our samples have velocity dispersion measurement data

(sigma) in Shen et al (2008). The masses of all NSL1 are well below, but become more very close to, the predictions of the M-sigma relation before and after the correction. The effect of the correction is obvious, albeit small number statistics due to the limited sample.

## 4 THE LOCATION OF THE IMLR AND THE EVIDENCES FOR ITS EXISTENCE

### 4.1 Broad Line Region evolution

We assume that both of the two regions (VBLR and IMLR) are bounded by the central black hole's gravity. Then, we have

$$f_1^2 \frac{V_{\text{VBLR}}^2}{R_{\text{VBLR}}} = \frac{GM_{\text{BH}}}{R_{\text{VBLR}}^2}, \quad (4)$$

and

$$f_2^2 \frac{V_{\text{IMLR}}^2}{R_{\text{IMLR}}} = \frac{GM_{\text{BH}}}{R_{\text{IMLR}}^2}. \quad (5)$$

These two equations lead to

$$R_{\text{IMLR}} = \left( \frac{f_1 V_{\text{VBLR}}}{f_2 V_{\text{IMLR}}} \right)^2 R_{\text{VBLR}} = C_0 \left( \frac{V_{\text{VBLR}}}{V_{\text{IMLR}}} \right)^2 R_{\text{VBLR}}, \quad (6)$$

where  $C_0 = \left( \frac{f_1}{f_2} \right)^2$ .  $C_0$  is a constant which need to be determined by further studies. The radius measured from reverberation is taken as  $R_{\text{VBLR}}$ . Therefore, we can calculate the radius of IMLR from the above equation.  $R_{\text{IMLR}}$  is proportional to  $C_0$ .  $C_0 = 1$  is used for all the calculation below.  $R_{\text{IMLR}}$  is obtained from H $\alpha$  and H $\beta$  lines separately. Fig.4 is the evolution of  $R_{\text{VBLR}}$  and  $R_{\text{IMLR}}$  with luminosity. The radius of the IMLR increases slower than VBLR with luminosity and black hole mass increasing. The two emission regions have a trend to merge into one with larger higher luminosity and black hole mass. as  $R_{\text{IMLR}} \propto L^{0.37 \pm 0.06}$  while  $R_{\text{VBLR}} \propto L^{0.52 \pm 0.04}$ .

### 4.2 The location of IMLR

The relation  $R_{\text{IMLR}} \propto L^{0.37 \pm 0.06}$  is consistent with the receding velocity of torus based on infrared reverberation mapping (Suganuma et al. 2006) and the receding velocity of torus that we can calculate based on analysis of type I AGN fraction (Simpson 2005). Our other analysis also shows that the IMLR may have higher density, more dusty than the VBGC, and the IMGC show slightly Baldwin effect while the VBGC does not. The Baldwin effect can be explained as a flattened geometry. These results suggest that IMLR is the inner hot skin of torus. A simple scenario of the BLR (BLR=VBLR+IMLR) evolution can be constructed as shown in Fig.5. The inner spherical region is the VBLR (Very Broad Line Region). It expands to a larger radius with luminosity increase and perhaps also black hole mass increase. IMLR is the inner part of the torus, which can be sublimated by the central radiation and thus its radius also increases with luminosity increase. When the luminosity is high enough, the broad line region and torus become one single entity, but with different physical conditions. This scenario is consistent with the dust bound BLR hypothesis which also showed that the delay time of infrared emission is always longer than the delay time of emission lines of

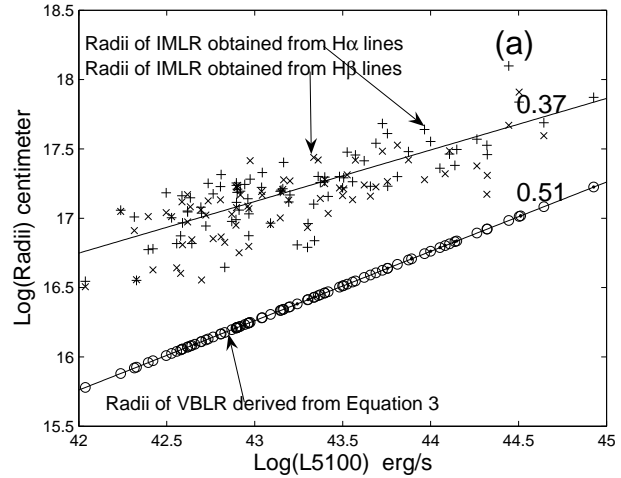


**Figure 4.** Correlation of the radii of IMLR and VBLR with luminosity. Circles are the VBLR radius,  $\times$  represent IMLR radius derived from H $\beta$  lines and  $+$  from H $\alpha$  lines. Circles filled with dots represent the objects missing the intermediate Gaussian component. The radius of the VBLR is obtained from the  $R_{\text{BLR}} \sim L^{0.51}$  (equation 2 not equation 3). These correlations supports a scenario of hierarchical evolution of AGNs.

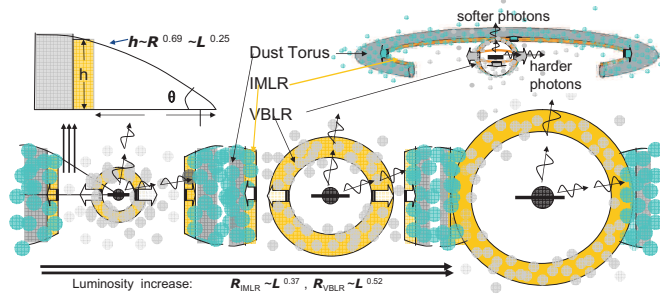


**Figure 5.** Cartoon of the Broad Line Region evolution. Continuum photons from the central region have slightly higher energies along the nearly edge-on direction. With black hole mass and luminosity increasing, both the VBLR and IMLR expand. The radius of VBLR increases faster, so the two regions have a trend to merge into one.

the corresponding AGN, but sometimes they are almost the same (Laor 2004; Elitzur 2006). Suganuma et al. (2006).

### 4.3 Evidence for the existence of IMLR

The first concrete evidence comes from the the study of the micro-lensing of the Broad Line Region in the lensed quasar J1131-1231 (Sluse et al. 2007, 2008). In this work they found evidence that the H $\beta$  emission line (as well as H $\alpha$ ) is differentially microlensed, with the broadest component (FWHM 4000 km/s) being much more micro-lensed than the narrower component (FWHM 2000 km/s). Because the amplitude of micro-lensing depends on the size of the emitting region, this is a clear evidence that the broadest compo-

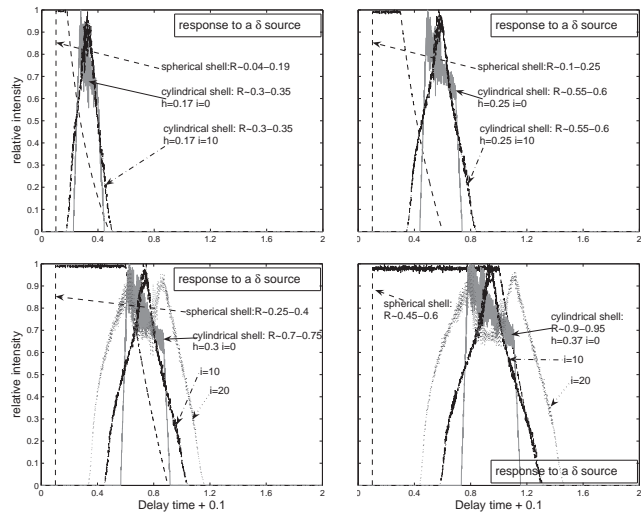


**Figure 6.** Different responses of different geometries to a delta impulse. The VBLR is assumed to be a spherical shell of uniform density, and the IMLR is assumed to be a cylindrical shell of uniform density. Time is normalized to arbitrary unit. Each figure shows a different  $R_{\text{IMLR}} - R_{\text{VBLR}}$  pair. Clearly in all cases the responses of IMLR have shorter variability and thus will result in narrower RMS spectra than that from VBLR.

ment of the emission line is more compact than the narrower component.

Then, we turn to the reverberation mapping experiment. If the IMLR is really a discrete emission region apart from the VBLR, another peak corresponding to the radius of this region might appear in the cross correlation function between the lightcurves of the emission line and the continuum. In fact, a possible example exists in the database of reverberation mapping observations (Peterson et al. 1998; 2004). Mrk 79 shows obviously double peaks in the cross correlation centroid distribution which has not been explained well so far which can be well explained in our model (please refer to Zhu et al. 2008 for details).

Another fact known to us is that the RMS spectrum of the broad emission line is normally (but not always) narrower systematically than the mean spectrum (Collin et al. 2006). If the emission lines are produced from two distinct regions, VBLR and IMLR, they will respond to the central continuum radiation differently. Because the IMLR has a flattened geometry, it can create a narrower response function to a delta impulse even with radius much larger than the VBLR, which is confirmed by our calculations shown in Fig.6.

## 5 SUMMARY

We conclude that the broad  $H\beta$ ,  $H\alpha$ , and  $H\gamma$  line of the AGNs in our sample can be well fitted by a double Gaussian model, i.e., VBGC and IMGC. The properties of the two components indicate that the two Gaussian components originate from two emission regions, i.e. VBLR and IMLR. The physical properties of IMLR suggest it should be the torus inner boundary region. Based on our model, The black hole mass measured by RM should be corrected, after cor-

rection the NLS1 follows M-sigma relation as well as BLS1. Therefore the problem of under-massive black hole in NLS1s appears to have disappeared. Our results offer strong evidence of the evolution of the broad line region (consists of a IMLR and a VBLR) from NLS1s to BLS1s in the hierarchical evolution scenario.

Finally, we show that the study of micro-lensing provide concrete evidence for the existence of IMLR and Mrk 79 provides possible evidence. Narrower RMS spectrum also support our model. The existence of a weak intermediate Gaussian component in the broad emission lines of many sources with reverberation mapping measurements may cause systematic biases for the measurements of the radius of the VBLR, It will be helpful to decompose each broad emission line into two Gaussian components as we have done here, and then do cross-correlation analysis between the continuum and each of the two components, in order to measure the Radius-Luminosity relations for the two components independently. This would provide decisive test for our model presented in this paper, as well as providing more accurate measurements of the masses of supermassive black holes in AGNs.

## ACKNOWLEDGMENT

We are extremely grateful to G. La Mura and L.C. Popovic for sending us the processed spectra we used in this work. SNZ thanks Jianmin Wang for many discussions, as well as sharing their early results which motivated us to pursue the work presented here. SNZ acknowledges partial funding support by Directional Research Project of the Chinese Academy of Sciences under project No. KJCX2-YW-T03 and by the National Natural Science Foundation of China under grant Nos. 10521001, 10733010, 10725313, and by 973 Program of China under grant 2009CB824800.

## REFERENCES

- Bentz, M.C., et al. 2006, ApJ, 644, 133
- Collin, S., Kawaguchi, T., Peterson, B.M., & Vestergaard, M. 2006, A&A, 456, 75
- Elitzur, M. 2006, ASP Conference Series, Vol.\*\*\*, Xi'an, China, 16-21 October, 2006
- Greene, J.E. & Ho, L.C. 2005, ApJ, 630, 122
- La Mura, G., et al. 2007, ApJ, 671, 104
- Laor, A. 2004, AGN Physics with the Sloan Digital Sky Survey, ASP Conference Series, 311, 169
- Magorrian, J., et al. 1998, AJ, 115, 2285
- Peterson, B.M., et al. 1998, ApJ, 501, 82
- Peterson, B.M., et al. 2004, ApJ, 613, 682
- Simpson, C. 2005, MNRAS, 360, 565
- Simpson, C. 2005, MNRAS, 360, 565
- Shen, J.J., et al. 2008, AJ, 135, 928
- Sluse, D., et al 2007, A&A, 468, 885
- Sluse, D., et al 2008, RMxAC, 32, 83
- Suganuma, M., et al. 2006, ApJ, 639, 46
- Tremaine, S., et al. 2002, ApJ, 574, 740
- Wang, T., & Lu, Y. 2001, AAP, 377, 52
- Zhou, H., Wang, T., Yuan, W., Lu, H., Dong, X., Wang, J., & Lu, Y. 2006, APJS, 166, 128
- Zhu, L., Zhang, S.N., & Tang, S.M. 2008, submitted to ApJ (arXiv:0807.3992)